Damping of magnetohydrodynamic disturbances in multi-ion-species plasmas

Mieko Toida,[a] Takashi Yoshiya, and Yukiharu Ohsawa
Department of Physics, Nagoya University, Nagoya 464-8602, Japan

(Received 15 November 2005; accepted 27 February 2006; published online 18 April 2006)

The evolution of macroscopic magnetohydrodynamic disturbances across a magnetic field is studied, with particular attention to the effect of multiple ion species. Analyses are carried out on disturbances where the initial magnetic profiles are sinusoidal. Both the theory and electromagnetic simulations show that, in a single-ion-species plasma, the disturbance is undamped, with its energy oscillating between the magnetic field and ion velocity. In a multi-ion-species plasma, however, it is initially damped, owing to the phase mixing of the magnetosonic mode and the modes having ion-ion hybrid cutoff frequencies. Furthermore, it is found from long-time simulations that the amplitude of the disturbance continues to decrease in a multi-ion-species plasma. This is due to nonlinear mode couplings. The magnetic energy is irreversibly transferred to the ions.
© *2006 American Institute of Physics*. [DOI: 10.1063/1.2188404]

I. INTRODUCTION

The presence of multiple ion species significantly influences wave propagation.[1–11] For instance, nonlinear magnetosonic pulses are damped in a multi-ion-species plasma, even if they propagate perpendicular to a magnetic field.[6,7] The damping is caused by the energy transfer from the pulses to heavy ions.[10]

In Ref. 12, the collective behavior of perpendicular ion Bernstein waves was studied, with attention to the effect of multiple ion species. In a single-ion-species plasma, the autocorrelation function $C_k(\tau)$ of a quasimode[13] consisting of ion Bernstein waves with a wave number k and frequencies $\omega \simeq n\Omega_i$, where n is integers and Ω_i is the ion gyrofrequency, exhibits quasiperiodic behavior with ion gyroperiod $2\pi/\Omega_i$. Although $C_k(\tau)$ is initially damped, owing to the phase mixing of many harmonic waves,[13,14] it almost returns to the initial value at $t=2\pi/\Omega_i$. In a multi-ion-species plasma with many different Ω_i's, however, the recurrence time of $C_k(\tau)$ should be extremely long; practically, $C_k(\tau)$ will not be recovered to its initial value. Particle simulations have also demonstrated that in a multi-ion-species plasma, macroscopic electrostatic disturbances are damped.

The above study was on short-wavelength ($k\rho_i \gg 1$), electrostatic fluctuations, where ρ_i is the ion gyroradius. Recently, long-wavelength ($k\rho_i \ll 1$), electromagnetic fluctuations in thermal-equilibrium, multi-ion-species plasmas have been studied.[15] In the frequency regime lower than the lower hybrid frequency ω_{LH}, there exist three types of modes, which we call the magnetosonic, ion cyclotron, and heavy-ion cutoff modes. The magnetosonic mode has frequencies $\omega \simeq kv_{\mathrm{A}}$ in the long-wavelength limit. Here, v_{A} is the Alfvén speed in a multi-ion-species plasma,

$$v_{\mathrm{A}} = B_0 \Big/ \left(4\pi \sum_i n_i m_i\right)^{1/2}, \tag{1}$$

where B_0 is the strength of the external magnetic field, and n_i and m_i are the ion density and mass, respectively. The ion cyclotron modes have frequencies near $n\Omega_i$.[16] The frequencies of the heavy-ion cutoff modes are given as

$$\omega_{s0} = \Omega_s + \frac{\omega_{ps}^2}{\Omega_s} \frac{1}{\sum_{i\neq s} \omega_{pi}^2/[\Omega_i/(\Omega_i - \Omega_s)]}, \tag{2}$$

where the subscript s denotes a heavy-ion species and ω_{pi} is the plasma frequency for the ion species i. [In Ref. 9, the frequencies (2) were called ion-ion hybrid cutoff frequencies.] The power spectra of thermal magnetic fluctuations of these modes were also analytically and numerically obtained. In a single-ion-species plasma, the magnetosonic mode is an overwhelmingly dominant mode. The autocorrelation function $C_k(\tau)$ is thus given by a cosine function with a constant amplitude. In a multi-ion-species plasma, however, the amplitudes of the heavy-ion cutoff modes can be comparable to that of the magnetosonic mode if kv_{A} is of the order of ω_{s0}. Therefore, $C_k(\tau)$ is initially damped, owing to the phase mixing of the magnetosonic and heavy-ion cutoff modes, and its recurrence time becomes quite long. This suggests that heavy-ion cutoff modes can significantly influence energy transport.

In this paper, by using particle simulations, we study low-frequency ($\omega \ll \omega_{\mathrm{LH}}$) evolution of macroscopic magnetohydrodaynamic disturbances and the associated energy transport. It is shown that the heavy-ion cutoff modes can cause the damping of macroscopic disturbances and the increase in ion kinetic energy.

We consider a one-dimensional initial value problem, where at time $t=0$, the magnetic field has a sinusoidal disturbance with a wave number k_0, while other quantities have no macroscopic disturbances; the wave number k_0 is assumed to be $k_0 v_{\mathrm{A}} < \Omega_a$, where Ω_a is the gyrofrequency of the

[a]Electronic mail: toida@cc.nagoya-u.ac.jp

 © 2006 American Institute of Physics

Downloaded 20 Sep 2007 to 133.6.32.11. Redistribution subject to AIP license or copyright, see http://pop.aip.org/pop/copyright.jsp

majority-species ions. In Sec. II, using a linear kinetic theory based on the Vlasov and Maxwell equations, we derive an equation for the time variation of the Fourier component $B_{k_0}(t)$ of the magnetic fields. It is shown that $B_{k_0}(t)$ has the same time dependence as the autocorrelation function $C_{k_0}(t)$ of thermal magnetic fluctuations. In a single-ion-species plasma, $B_{k_0}(t)$ oscillates with a frequency $\omega \simeq k_0 v_A$ and is undamped. In a multi-ion-species plasma, however, $B_{k_0}(t)$ is initially damped because of the phase mixing of the magnetosonic and heavy-ion cutoff modes.

With particle simulations, we verify the linear theory for the initial damping in Sec. III. Further, we perform long-time simulations until $\Omega_a t = 1400$ and show that $B_{k_0}(t)$ is not recovered in the multi-ion-species plasma. In the early stage, $\Omega_a t < 100$, the behavior of $B_{k_0}(t)$ agrees with the prediction of the linear theory. Later, $\Omega_a t > 300$, however, $B_{k_0}(t)$ in the simulation continues to be damped, and $|B_{k_0}(t)|$ in the simulation finally becomes much smaller than that in the linear theory. This damping is due to nonlinear mode couplings; from the magnetosonic and heavy-ion cutoff modes with the wave number k_0, many different waves with $k \neq k_0$ are generated. In association with this damping, ion kinetic energy increases. The energy transfer is enhanced when $k_0 v_A \sim \omega_{s0}$.

II. THEORY

We consider a one-dimensional ($\partial/\partial y = \partial/\partial z = 0$), initial value problem for electromagnetic perturbations. The electric field $\boldsymbol{E}(x,t)$ is zero at $t=0$, while the magnetic field $B_z(x,t)$ has a sinusoidal disturbance with a wave number k_0,

$$\delta B_z(x,0) \equiv B_z(x,0) - B_0 = B_{k_0}(0)\cos(k_0 x), \tag{3}$$

in an external magnetic field, $\boldsymbol{B}_0 = (0,0,B_0)$. The ions and electrons have Maxwellian velocity distribution functions with temperatures T_i and T_e, respectively. We study low-frequency ($|\omega| \ll \omega_{LH}$) evolution of this disturbance.

From the linearized Maxwell and Vlasov equations, we find the time variation of the Fourier component $B_{k_0}(t)$ for $t > 0$ as (see the Appendix)

$$\frac{B_{k_0}(t)}{B_{k_0}(0)} = \sum_n b(k_0, \omega_n)\exp(-i\omega_n t), \tag{4}$$

with

$$b(k_0,\omega) = \frac{c^2 k_0^2}{\omega^3}\frac{\epsilon_{xx}}{\partial|D|/\partial\omega}, \tag{5}$$

where ω_n is a root of the equation

$$|D| = \varepsilon_{xx}(\varepsilon_{yy} - c^2 k_0^2/\omega^2) + \varepsilon_{xy}^2 = 0. \tag{6}$$

The quantities ε_{xx}, ε_{xy}, and ε_{yy} are the components of the dielectric tensor; their specific forms are given in the Appendix . In a multi-ion-species plasma, Eq. (6) gives three types of modes in the low-frequency ($|\omega| \ll \omega_{LH}$) regime; the magnetosonic mode with $\omega \simeq \pm k_0 v_A$, ion-cyclotron modes with $\omega \simeq \pm n\Omega_i$, and heavy-ion cutoff modes with $\omega \simeq \pm \omega_{s0}$.

The quantity $b(k_0,\omega)$ is related to the power spectrum of magnetic fluctuations in a thermal equilibrium plasma, $P_{k_0}(\omega)$, as

$$b(k_0,\omega) = P_{k_0}(\omega)/(\pi k_B T) \tag{7}$$

[see Eq. (24) of Ref. 15]. Thus, $B_{k_0}(t)$ has the same time dependence as the autocorrelation function $C_{k_0}(t)$ of thermal magnetic fluctuations.

We can therefore use the results of the calculations of thermal fluctuations[15] to obtain $b(k_0,\omega)$. In thermal equilibrium, the amplitudes of the magnetosonic and heavy-ion cutoff modes are given as

$$P_{k_0}(k_0 v_A)/(\pi k_B T) \sim 1/2, \tag{8}$$

$$P_{k_0}(\omega_{s0})/(\pi k_B T) \sim \frac{1}{2}\frac{\omega_{ps}^2 \Omega_H^2}{\omega_{pH}\Omega_s^4}(\Omega_H - \Omega_s)^2 c^2 k^2. \tag{9}$$

If $k_0 \rho_i \ll 1$, the amplitudes of the ion-cyclotron modes, $P_{k_0}(n\Omega_i)$, are much smaller than $P_{k_0}(k_0 v_A)$.[15] In a single-ion-species plasma, where heavy-ion cutoff modes do not exist, therefore, the magnetosonic mode $P_{k_0}(k_0 v_A)$ is dominant. From these properties of $P_{k_0}(\omega)$, we find the ω dependence of $b(k_0,\omega)$. We thus obtain, from Eq. (4), $B_{k_0}(t)$ in a single-ion-species plasma as

$$B_{k_0}(t)/B_{k_0}(0) \sim \cos(k_0 v_A t). \tag{10}$$

This disturbance is undamped. In a multi-ion-species plasma, however, $P_{k_0}(\omega_{s0})$ can be comparable to $P_{k_0}(k_0 v_A)$ if $k_0 v_A \sim \omega_{s0}$. As a result, $C_{k_0}(t)$ is initially damped, owing to the phase mixing of these modes, and recurrence will not occur practically. The behavior of $B_{k_0}(t)$ is the same as that of $C_{k_0}(t)$.

To see the irreversibility, we examine the value of $B_{k_0}(t)$ at time $t = 2n\pi/(k_0 v_A)$, where n is an integer. Equation (4) gives

$$\frac{B_{k_0}[2n\pi/(k_0 v_A)]}{B_{k_0}(0)} \sim 1 - \sum_s b(k_0,\omega_{s0})\sin^2\left(\frac{\pi n \omega_{s0}}{k_0 v_A}\right). \tag{11}$$

The first and second terms on the right-hand side are due to the magnetosonic and heavy-ion cutoff modes, respectively. Equation (11) becomes unity only if $(n\omega_{s0}/kv_A)$'s are all integers. In order for this to occur, (ω_{s0}/kv_A)'s must be all rational numbers, which is quite unlikely. Even if this occurs, the values of n must be huge if there are many kinds of ions. The recurrence time of $B_{k_0}(t)$ should thus be extremely long; $B_{k_0}(t)$ would disappear before the recurrence, owing to collisions or some nonlinear effects. Practically, therefore, the damping of $B_{k_0}(t)$ will be irreversible in a multi-ion-species plasma.

III. SIMULATION STUDIES OF THE EVOLUTION OF MACROSCOPIC DISTURBANCES

A. Method and parameters

We now use a one-dimensional (one space coordinate and three velocity components) electromagnetic particle code with full ion and electron dynamics to study the evolution of macroscopic magnetic disturbances and associated energy transport.

Downloaded 20 Sep 2007 to 133.6.32.11. Redistribution subject to AIP license or copyright, see http://pop.aip.org/pop/copyright.jsp

We simulate single- and four-ion-species plasmas; we denote the ion species in the former by a and those in the latter by a, b, c, and d. The electric charges are assumed to be the same, $q_a=q_b=q_c=q_d=|q_e|$. To make the computational time short, we take small ion-to-electron mass rations. The ratio of the lightest ion mass to the electrons mass is $m_a/m_e=50$. The ion mass ratios are set to be $m_b/m_a=\sqrt{3}$, $m_c/m_a=2$, and $m_d/m_a=\sqrt{5}$. In order to see the effect of multiple ion species with a small number of ion species, we have chosen the irrational ion mass ratios for b and d ions. [That is, if the ion mass rations are rational, as mentioned later, Eq. (11), the recurrence could occur in a system with a small number of ion species, even though the recurrence time becomes extremely long in a system with a large number of ion species.] The ion densities are set to be $n_b=n_c=n_d=0.2n_a$. The total number of electrons is $N_e\simeq 4.2\times 10^6$. The electrons and ions initially have Maxwellian velocity distribution functions. All the ion species have the same temperature, T_i with $T_i/T_e=0.1$.

We use periodic boundary conditions with periodicity $L_x=4096\,\Delta_g$, where Δ_g is the grid spacing. The normalized speed of light is $c/(\omega_{pe}\Delta_g)=4$. The normalized thermal velocity of electrons is $v_{Te}/(\omega_{pe}\Delta_g)=1$. The collisional energy relaxation time between the (finite sized) electrons and ions[17] is $\omega_{pe}\tau_c\sim 10^7$.

The external magnetic field is in the z direction with $|\Omega_e|/\omega_{pe}=4.0$. Then, the Alfvén speeds in the single- and four-ion-species plasmas are $v_A/(\omega_{pe}\Delta_g)=2.3$ and 2.0, respectively. The beta value (the ratio of kinetic to magnetic energy densities) is 0.008. The heavy-ion cutoff frequencies are $\omega_{b0}/\Omega_a\simeq 0.69$, $\omega_{c0}/\Omega_a\simeq 0.52$, and $\omega_{d0}/\Omega_a\simeq 0.46$.

As in the theory, the magnetic field initially has a sinusoidal disturbance given by Eq. (3) with an amplitude $B_{k_0}(0)/B_0=0.04$ and wave number $k_0\Delta_g=0.025$; the values of k_0v_A/Ω_a in the single- and four-ion-species plasmas are then 0.70 and 0.60, respectively. Other physical quantities have no macroscopic disturbances at $t=0$.

In the theory, the frequencies of fluctuations have been assumed to be low, $\omega\ll\omega_{LH}$. The present simulations, however, include high-frequency fluctuations such as electromagnetic waves with $\omega\geqslant\omega_{pe}$ as well as low-frequency ones. Also, nonlinear processes such as mode couplings can develop in the simulations. All the processes are treated self-consistently. That is, the simulation covers a wider area of plasma physics than the present theory. We thus use the simulations to test the theory.

B. Simulation results

We first present the results of short-time simulations, such that $\Omega_a t\leqslant 120$ and examine the initial damping. Next, we will show long-time simulations until $\Omega_a t=1400$ and study energy transport.

1. Short-time evolution

Figure 1 shows the profiles of B_z-B_0 at five different times in the single-ion-species plasma. There is a standing wave oscillating with a period $t'\equiv k_0v_At/\pi=2.0$; at this time, both the profile and amplitude return to their initial ones.

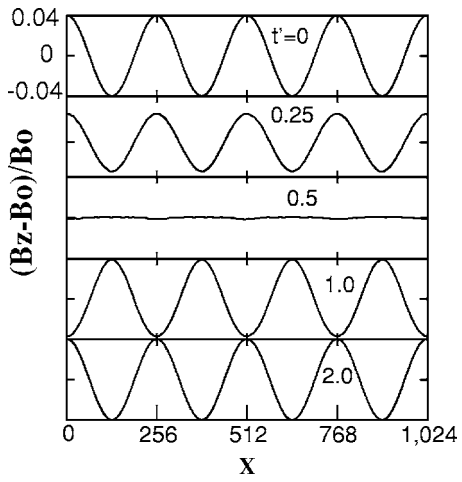

FIG. 1. Profiles of B_z in the single-ion-species plasma at times $t'\simeq k_0v_At/\pi=0$, 0.25, 0.5, 1.0, and 2.0.

Figure 2 shows B_z profiles in the four-ion-species plasma. Here, the amplitude is not recovered to the initial value, even at the times of $t'=k_0v_At/\pi=1.0$ and 2.0.

Figure 3 shows time variations of the Fourier component $B_{k_0}(t)$ in the single- and four-ion-species plasmas. The dots are the simulation results, while the solid lines represent the theory (4). The simulation results fit well to the theoretical lines. In the single-ion-species plasma, $B_{k_0}(t)$ oscillates with the frequency $\omega\simeq k_0v_A$ without damping. In the four-ion-species plasma, $B_{k_0}(t)$ is initially damped, and then the amplitude $|B_{k_0}(t)|$ remains to be smaller than the initial one. The damping is due to the phase mixing of the magnetosonic mode and heavy-ion cutoff modes; the power spectra of magnetic fields will be shown in the next section.

We show in Fig. 4 time variations of magnetic perturbation energy,

$$E_B=\int dx(B_z-B_0)^2/(8\pi)=L_x\sum_k|B_k|^2/(8\pi), \tag{12}$$

and of the change in ion kinetic energy, $\Delta E_i=E_i-E_{i0}$, where E_i is the total ion kinetic energy, and E_{i0} is its initial one. The

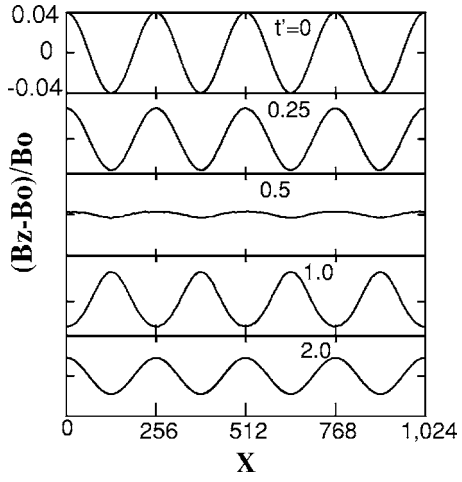

FIG. 2. Profiles of B_z in the four-ion-species plasma at times $t'\simeq k_0v_At/\pi=0$, 0.25, 0.5, 1.0, and 2.0.

Downloaded 20 Sep 2007 to 133.6.32.11. Redistribution subject to AIP license or copyright, see http://pop.aip.org/pop/copyright.jsp

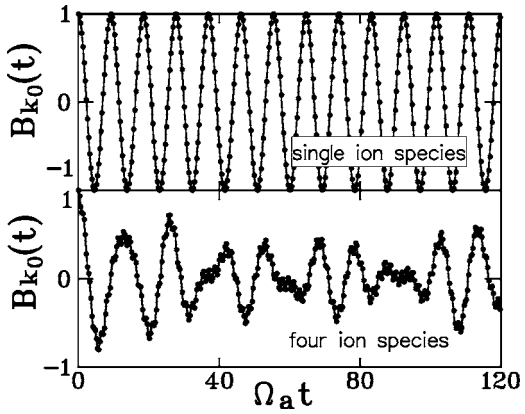

FIG. 3. Time variations of the Fourier component $B_{k_0}(t)$ in the single- and four-ion-species plasmas. The dots and solid lines represent the simulation results and the theory, Eq. (4), respectively. The values of $B_{k_0}(t)$ are normalized to its initial value $B_{k_0}(0)$.

energies are normalized to $m_e v_{Te}^2$. The gray and black lines represent energies in the single- and four-ion-species plasmas, respectively. In the former plasma, both the magnetic and ion energies oscillate with the period $k_0 v_A t = \pi$. In the latter plasma, the magnetic perturbation energy decreases, giving nearly the same amount to the ion kinetic energy.

2. Long-time evolution of magnetic fields

We now study the same initial value problem for a much longer time ($\Omega_a t = 1400$). In the single-ion-species plasma, $B_{k_0}(t)$ is undamped even in this case; we do not show its profile here because it is quite similar to the top panel of Fig. 3. In the four-ion-species plasma, however, $B_{k_0}(t)$ is not recovered, as shown in Fig. 5. In the early stage, $\Omega_a t < 150$, the simulation result (the black line) is in good agreement with the linear theory (the gray line). However, for $\Omega_a t > 300$, $|B_{k_0}(t)|$ of the simulation keeps decreasing and becomes much smaller than that of the linear theory (4).

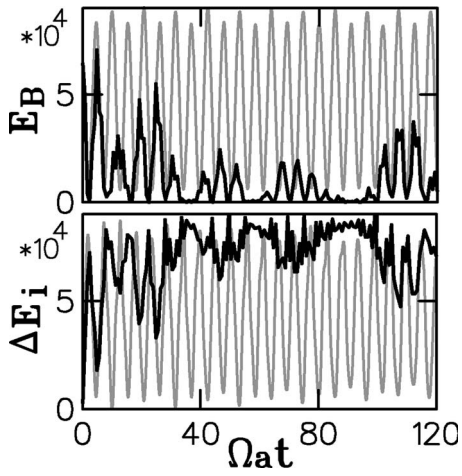

FIG. 4. Time variations of magnetic perturbation energies and ion kinetic energies, $\Delta E_i = E_i - E_{i0}$. The gray and black lines show energies in the single- and four-ion-species plasmas, respectively. The energies are normalized to $m_e v_{Te}^2$.

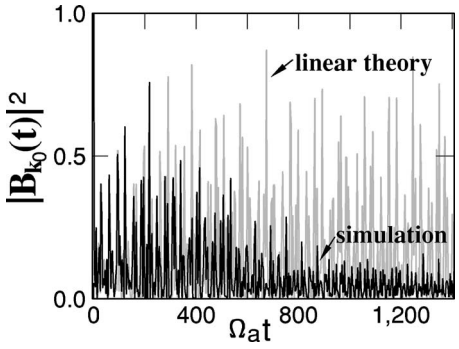

FIG. 5. The long-time evolution of $|B_{k_0}(t)|^2$ in the four-ion-species plasma. The black and gray lines represent the simulation result and the theory, Eq. (4), respectively.

The damping of $|B_{k_0}(t)|$ in the long-time simulation is not due to any numerical instabilities. The total energy in the simulation is well conserved; its increase is only 0.08%. In addition, as mentioned previously, $B_{k_0}(t)$ is undamped in the simulation of the single-ion-species plasma.

We show in Figs. 6 and 7 the power spectra of magnetic fields with $k = k_0$ in the single- and four-ion-species plasmas, respectively. The upper panels show spectra $P_1(k_0, \omega)$ in the early stage, $0 < \Omega_a t < 700$, while the lower ones show spectra $P_2(k_0, \omega)$ for $700 < \Omega_a t < 1400$. In the single-ion-species plasma, P_1 and P_2 have two peaks at $\omega \simeq \pm k_0 v_A$, and the peak values of P_1 and P_2 are nearly the same. In the four-ion-species plasma, we find several peaks at $\omega \simeq \pm k_0 v_A$ and near heavy-ion cutoff frequencies, $\pm\omega_{b0}$, $\pm\omega_{c0}$ and $\pm\omega_{d0}$; they are in the order $\omega_{d0} < \omega_{c0} < k_0 v_A < \omega_{b0}$. The peak values of P_2 are considerably smaller than those of P_1.

The damping of these k_0 modes is caused by nonlinear mode couplings. Figure 8 shows the contour map of increase in P, $dP(k, \omega) = P_2 - P_1$, in the (ω, k) plane. The four small circles indicate the positions of the original k_0 modes. The four vertical lines represent the lower hybrid frequency (line LH) and heavy-ion cutoff frequencies (lines b, c, d). We find that many waves are excited along the magnetosonic curve up to $\omega \sim \omega_{LH}$. Also, waves are generated near the heavy-ion

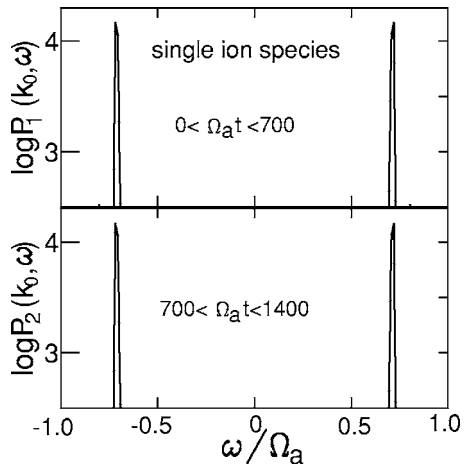

FIG. 6. Power spectra of magnetic fields with $k = k_0$ in the single-ion-species plasma. The upper and lower panels are for the periods $0 < \Omega_a t < 700$ and $700 < \Omega_a t < 1400$, respectively.

Downloaded 20 Sep 2007 to 133.6.32.11. Redistribution subject to AIP license or copyright, see http://pop.aip.org/pop/copyright.jsp

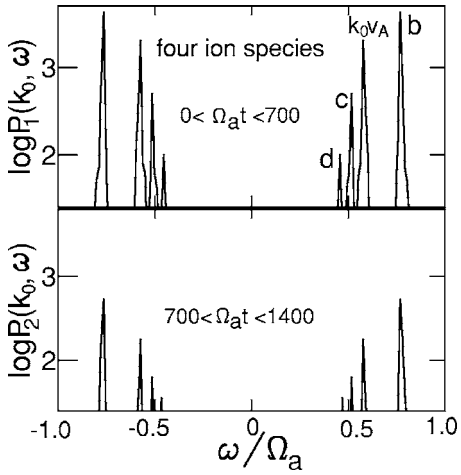

FIG. 7. The power spectra of magnetic fields with $k=k_0$ in the four-ion-species plasma. The heavy-ion cutoff frequencies are $\omega_{b0}/\Omega_a=0.69$, $\omega_{c0}/\Omega_a=0.52$, and $\omega_{d0}/\Omega_a=0.46$, while the frequency of the magnetosonic mode is $k_0v_A/\Omega_a=0.60$.

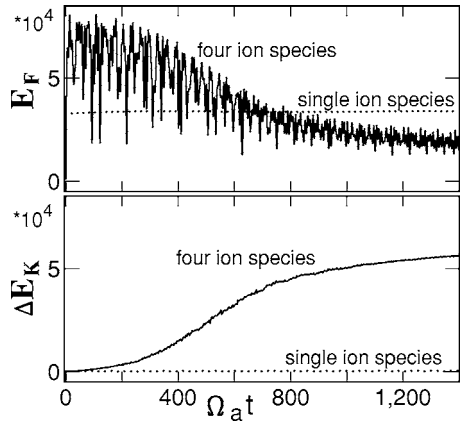

FIG. 9. Time variations of ion kinetic energies, E_F and E_K. The dashed and solid lines represent the energies in the single- and four-ion-species plasmas, respectively. The energy E_F of the single-ion-species plasma is averaged over the period $k_0v_At=2\pi$.

cutoff frequencies. In the single-ion-species plasma, dP is zero at nearly all the points. Even at the position of the maximum dP, the ratio $dP/P_1(k_0,k_0v_A)$ is of order 10^{-4}.

In the four-ion-species plasma, nonlinear mode couplings can excite many different waves from the original four modes with $k=k_0$, as shown in Fig. 8. For example, from the magnetosonic mode $(k_0,0.60\Omega_a)$ and c-ion cutoff mode $(k_0,0.52\Omega_a)$, a shorter wavelength magnetosonic mode $(2k_0,1.12\Omega_a)$ can be produced through a resonant three-wave coupling. This shorter wavelength mode can generate the mode $(3k_0,0.66\Omega_a)$ near the b-ion cutoff frequency with the coupling with the d-ion cutoff mode $(k_0,-0.46\Omega_a)$.

3. Energy transport to ions

We now investigate the time variation of ion kinetic energies. We examine two kinds of energies; fluid kinetic energy,

$$E_F=\sum_i \int dx\, m_i n_i(x)\langle \boldsymbol{v}_i(x)\rangle^2/2, \tag{13}$$

and kinetic energy in the local moving coordinate system,

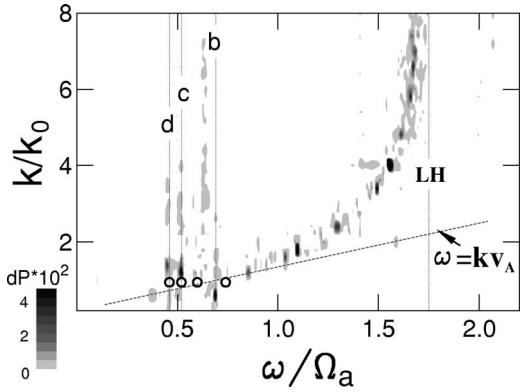

FIG. 8. An increase in P, $dP(k,\omega)=P_2(k,\omega)-P_1(k,\omega)$, in the four-ion-species plasma. The four vertical lines represent the lower hybrid resonance frequency and heavy-ion cutoff frequencies.

$$E_K=\sum_i \int dx \int d\boldsymbol{v}\, m_i f_i(x,\boldsymbol{v})\{\boldsymbol{v}-\langle \boldsymbol{v}_i(x)\rangle\}^2/2, \tag{14}$$

where the density $n_i(x)$ and fluid velocity $\langle \boldsymbol{v}_i(x)\rangle$ are defined as

$$n_i(x)=\int d\boldsymbol{v}\, f_i(x,\boldsymbol{v}), \tag{15}$$

$$\langle \boldsymbol{v}_i(x)\rangle=\int d\boldsymbol{v}\, f_i(x,\boldsymbol{v})\boldsymbol{v}/n_i(x). \tag{16}$$

Figure 9 shows time variations of E_F and of the change in E_K; $\Delta E_K=E_K(t)-E_K(0)$, where $E_K(0)=18\times10^4$. The dashed and solid lines are for the single- and four-ion-species plasmas, respectively. In the former, both E_F and E_K are almost constant, while, in the latter, the fluid energy E_F grows in the early stage, $\Omega_a t<100$, and then gradually decreases. The kinetic energy E_K keeps increasing. The values of E_F and E_K have both significantly changed by $\Omega_a t\sim800$, which is of the order of the damping time of $|B_{k_0}(t)|$ shown in Fig. 5. The damping of $|B_{k_0}(t)|$ and increase in E_K seems to be irreversible.

At $\Omega_a t=1400$, about 66% of the initial magnetic disturbance energy is transferred to the ion kinetic energy, E_K, and 22% to the ion fluid energy, E_F. The rest $(\sim10\%)$ of the initial disturbance energy is converted to the energies of magnetic and electric fields with $k\neq k_0$ through nonlinear mode couplings.

We show in Fig. 10 the energy distribution functions of ions, $f\{[\boldsymbol{v}-\langle \boldsymbol{v}_i\rangle]^2\}$ at $\Omega_a t=0$ and 1400. The distributions of minor heavy ions (b, c, and d ions) are noticeably broadened, while that of a ions, which are major, does not change much. The amount of energy gain depends on the ion species.

In the absence of mode couplings, E_k does not increase. To confirm this, we have performed a simulation where the electric and magnetic fields with $|k|>k_0$ are set to be zero. Figure 11 shows the time variations of $|B_{k_0}|^2$ (upper panel) and of E_F and E_K (lower panel) in the four-ion-species

Downloaded 20 Sep 2007 to 133.6.32.11. Redistribution subject to AIP license or copyright, see http://pop.aip.org/pop/copyright.jsp

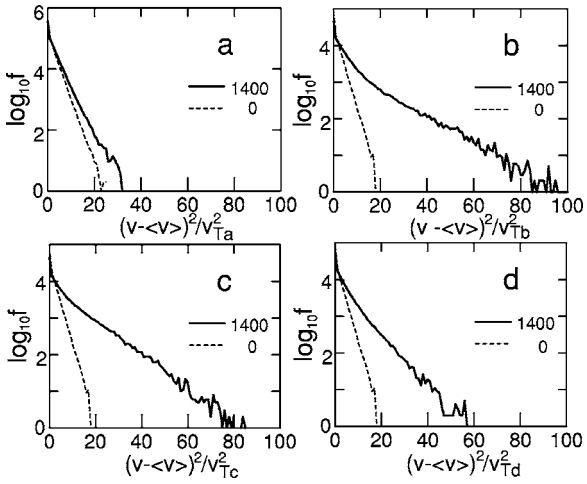

FIG. 10. Energy distribution functions of ions, $f[(\boldsymbol{v}-\langle \boldsymbol{v}_i \rangle)^2]$, at $\Omega_a t=0$ and 1400. Here, v_{Ti} ($i=a$, b, c, or d) is the initial thermal velocity.

plasma. The damping of $|B_{k0}|$ is not observed; $|B_{k_0}|$ is almost constant, on average. Also, $\Delta E_K = E_K(t) - E_k(0)$ is nearly zero.

4. Wave number dependence

To see how the energy transfer depends on the wave number k_0 of the initial disturbance, we have carried out many simulations with different k_0. Figure 12 shows the dependence of $\langle |B_{k_0}|^2 \rangle$ on the wave number k_0, where the brackets denote the average from $\Omega_a t=0$ to 400. In the single-ion-species plasma (denoted by line 1), $\langle |B_{k_0}|^2 \rangle$ depends little on k_0. This is because the magnetosonic mode is always dominant. In the two-ion-species plasma with $n_c/n_a = 0.2$ (line 2), $\langle |B_{k_0}|^2 \rangle$ becomes small when $k_0 v_A \sim \omega_{c0}$. In the four-ion-species plasma (line 4), where the density ratios as the same as those in Fig. 10, $\langle |B_{k_0}|^2 \rangle$ is small for many k_0's, indicating that energy transfer is enhanced for a wider region of k_0.

IV. SUMMARY

We have theoretically and numerically studied the low-frequency ($\omega \ll \omega_{LH}$) evolution of macroscopic electromagnetic disturbances across a magnetic field in a multi-ion-species plasma. In both theory and simulations, we have solved the initial value problem, in which the magnetic field has a sinusoidal disturbance with a wave number k_0 at $t=0$; the wave number is assumed to be $k_0 v_A \lesssim \Omega_a$.

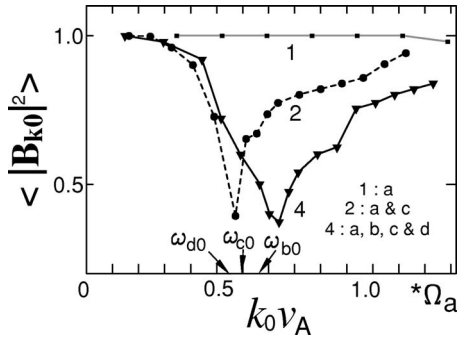

FIG. 12. Dependence of time-averaged $|B_{k_0}(t)|^2$ on the wave number k_0 and on the number of ion species. Here, $\langle |B_{k_0}(t)|^2 \rangle$ for three cases (single-, two-, and four-ion-species plasmas) are shown.

Using a linear kinetic theory, we have derived the equation for the time variation of $B_{k_0}(t)$ and have shown that $B_{k_0}(t)$ has the same time dependence as the autocorrelation function $C_{k_0}(t)$ of thermal magnetic fluctuations, which was given in Ref. 15. In a single-ion-species plasma, $B_{k_0}(t)$ is a cosine function with the frequency $\omega \simeq k_0 v_A$ and with a constant amplitude. In a multi-ion-species plasma, $B_{k_0}(t)$ is initially damped, owing to the phase mixing of the magnetosonic and heavy-ion cutoff modes.

With a one-dimensional electromagnetic particle code, we then studied the evolution of low-frequency disturbances and associated energy transport. In the single-ion-species plasma, $B_{k_0}(t)$ is undamped, as predicted by the theory. In the four-ion-species plasma, $B_{k_0}(t)$ in the simulation is in good agreement with the theory in the early stage, $\Omega_a t \lesssim 100$. In the later stage, $\Omega_a t > 300$, however, $|B_{k_0}(t)|$ in the simulation keeps decreasing and becomes much smaller than that in the linear theory. This damping is caused by nonlinear mode couplings, which generate many different waves with $k \neq k_0$ from the original magnetosonic and heavy-ion cutoff modes with $k=k_0$. As a result of these nonlinear processes, the ion kinetic energy E_K increases. (In a three dimensional system, the effects of nonlinear mode couplings would be more important.) The energy transfer to the ions is particularly enhanced when $k_0 v_A$ is of the order of the heavy-ion cutoff frequencies.

In the present work we indicate that the presence of multiple-ion species can enhance the energy transfer from magnetohydrodynamic disturbances to the ions. These processes could be important in the transport in, for instance, the solar corona, where the number of ion species is quite large and each ion species has many different ionic charge states.

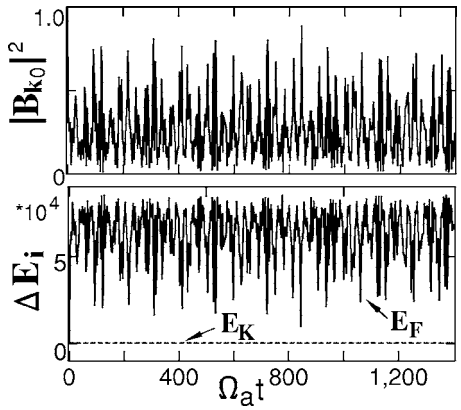

FIG. 11. Time variations of $|B_{k_0}|^2$ and ion kinetic energies E_F and E_K in the four-ion-species plasma. Electric and magnetic fields with $|k| > k_0$ are set to be zero.

ACKNOWLEDGMENTS

The numerical work was carried out by the joint research program, No. NIFS05KNXN032 and No. NIFS04KTAT003, of the National Institute for Fusion Science.

Downloaded 20 Sep 2007 to 133.6.32.11. Redistribution subject to AIP license or copyright, see http://pop.aip.org/pop/copyright.jsp

APPENDIX: DERIVATION OF $B_{k_0}(t)$

We make the Fourier-Laplace transformation of the linearized Maxwell and Vlasov equations; the Laplace transformation is defined as

$$\tilde{F}(\omega)=\int_0^\infty dt\,\exp(i\omega t)F(t),\quad \mathrm{Im}\,\omega>0. \tag{A1}$$

From the Maxwell equations, we have

$$-\frac{i\omega}{c}\tilde{\boldsymbol{E}}_{\boldsymbol{k}}(\omega)-\frac{1}{c}\boldsymbol{E}_{\boldsymbol{k}}(0)=i\boldsymbol{k}\times\tilde{\boldsymbol{B}}_{\boldsymbol{k}}(\omega)-\frac{4\pi}{c}\sum_j q_j n_{j0}\int d\boldsymbol{v}\,\boldsymbol{v}\,\delta\tilde{f}_{j\boldsymbol{k}}(\boldsymbol{v},\omega), \tag{A2}$$

$$\frac{i\omega}{c}\tilde{\boldsymbol{B}}_k(\omega)-\frac{1}{c}\boldsymbol{B}_{\boldsymbol{k}}(0)=i\boldsymbol{k}\times\tilde{\boldsymbol{E}}_{\boldsymbol{k}}(\omega), \tag{A3}$$

where $\boldsymbol{k}$ is the wave vector, $\boldsymbol{E}_{\boldsymbol{k}}(0)$ and $\boldsymbol{B}_{\boldsymbol{k}}(0)$ are the initial, Fourier transformed, electric and magnetic fields, and $\delta\tilde{f}_{j_{\boldsymbol{k}}}(\boldsymbol{v},\omega)$ is the Fourier-Laplace transformation of the perturbation of velocity distribution function, $\delta f_j(\boldsymbol{x},\boldsymbol{v},t)=f_j(\boldsymbol{x},\boldsymbol{v},t)-f_{j0}(\boldsymbol{v})$. From the Vlasov equation, we find $\delta f_j(\boldsymbol{x},\boldsymbol{v},t)$ as

$$\delta f_j(\boldsymbol{x},\boldsymbol{v},t)=\delta f_j(\boldsymbol{x},\boldsymbol{v},0)-\frac{q_j}{m_j}\int_0^t dt'\,\boldsymbol{E}[\boldsymbol{x}(t'),t]\cdot\frac{\partial f_{j0}(\boldsymbol{v})}{\partial\boldsymbol{v}}. \tag{A4}$$

Here, we carry out the integration along the unperturbed particle orbit.

As initial conditions, we assume that

$$\boldsymbol{E}_{\boldsymbol{k}}(0)=0,\delta f_j(\boldsymbol{x},\boldsymbol{v},0)=0. \tag{A5}$$

The equilibrium velocity distribution function $f_{j0}(\boldsymbol{v})$ is Maxwellian; using the dielectric tensor ε, Eq. (A2) is then written as[18]

$$-\frac{c}{\omega}\boldsymbol{k}\times\tilde{\boldsymbol{B}}_k(\omega)=\varepsilon\cdot\tilde{\boldsymbol{E}}_k(\omega). \tag{A6}$$

For low-frequency ($|\omega|\ll\omega_{\mathrm{LH}}$) waves propagating in the x direction in a magnetic field in the z direction, the components of the dielectric tensor become

$$\varepsilon_{xx}=1+\frac{\omega_{pe}^2}{\Omega_e^2}-\sum_i\sum_{n=1}^\infty\frac{2\omega_{pi}^2}{(\omega^2-n^2\Omega_i^2)}\frac{n^2}{\mu_i}\Gamma_n(\mu_i), \tag{A7}$$

$$\varepsilon_{xy}=-i\frac{\omega_{pe}^2}{\omega|\Omega_e|}-i\sum_i\sum_{n=1}^\infty\frac{2\omega_{pi}^2}{\omega(\omega^2-n^2\Omega_i^2)}n^2\Gamma_n'(\mu_i), \tag{A8}$$

$$\varepsilon_{yy}=\varepsilon_{xx}+\sum_i\sum_{n=1}^\infty\frac{4\omega_{pi}^2}{(\omega^2-n^2\Omega_i^2)}\mu_i\Gamma_n'(\mu_i)+\sum_i\frac{2\omega_{pi}^2}{\omega^2}\mu\Gamma_0'(\mu_i), \tag{A9}$$

where the subscript i refers to the ion species, $\mu_i=k^2\rho_i^2$, and $\Gamma_n(\mu_i)=I_n(\mu_i)\exp(-\mu_i)$ with I_n the modified Bessel function of the nth order.

The electric fields of low-frequency waves with the wave vector $\boldsymbol{k}=(k_0,0,0)$ have the x and y components, while the magnetic fields have only the z component; $\boldsymbol{E}_{\boldsymbol{k}}=(E_{xk_0},E_{yk_0},0)$ and $\boldsymbol{B}_{\boldsymbol{k}}=(0,0,B_{k_0})$. By use of the dispersion tensor D

$$D=\begin{pmatrix}\varepsilon_{xx}, & \varepsilon_{xy}\\ -\varepsilon_{xy}, & \varepsilon_{yy}-c^2k_0^2/\omega^2\end{pmatrix}, \tag{A10}$$

Eqs. (A3) and (A6) are reduced to

$$D\begin{pmatrix}\tilde{E}_{xk_0}(\omega)\\ \tilde{E}_{yk_0}(\omega)\end{pmatrix}=-\frac{ck_0}{i\omega^2}\begin{pmatrix}0\\ B_{k_0}(0)\end{pmatrix}. \tag{A11}$$

It then follows that

$$\tilde{E}_{yk_0}(\omega)=i\frac{ck_0}{\omega^2}\frac{\varepsilon_{xx}}{|D|}B_{k_0}(0), \tag{A12}$$

where $|D|$ is the determinant of D. From Eqs. (A3) and (A12), we find $\tilde{B}_{k_0}(\omega)$ as

$$\tilde{B}_{k_0}(\omega)=i\left(\frac{\varepsilon_{xx}\varepsilon_{yy}+\varepsilon_{xy}^2}{\omega|D|}\right)B_{k_0}(0). \tag{A13}$$

The inverse Laplace transformation of Eq. (A13) gives $B_{k_0}(t)$ for $t>0$ as

$$B_{k_0}(t)=\sum_n\left(\frac{\varepsilon_{xx}\varepsilon_{yy}+\varepsilon_{xy}^2}{\omega\partial|D|/\partial\omega}\right)\delta(\omega-\omega)\exp(-i\omega_n t)B_{k_0}(0), \tag{A14}$$

where ω_n is a root of $|D|=0$. Using Eq. (6), we rewrite Eq. (A14) as Eq. (4).

[1] S. J. Buchsbaum, Phys. Fluids **3**, 418 (1960).
[2] A. B. Mikhailovskii and A. I. Smolyakov, Sov. Phys. JETP **61**, 109 (1985).
[3] U. Motschmann, K. Sauer, T. Roatsch, and J. F. Mckenzie, J. Geophys. Res. **96**, 13841 (1991).
[4] M. Toida and Y. Ohsawa, J. Phys. Soc. Jpn. **63**, 573 (1994).
[5] S. Boldyrev, Phys. Lett. A **204**, 386 (1995).
[6] D. Dogen, M. Toida, and Y. Ohsawa, Phys. Plasmas **5**, 1298 (1998).
[7] M. Toida, D. Dogen, and Y. Ohsawa, J. Phys. Soc. Jpn. **68**, 2157 (1999).
[8] S. Irie and Y. Ohsawa, Phys. Plasmas **10**, 1253 (2003).
[9] G. W. Watson, W. W. Heidbrink, K. H. Burrell, and G. J. Kramer, Plasma Phys. Controlled Fusion **46**, 471 (2004).
[10] M. Toida and Y. Ohsawa, J. Phys. Soc. Jpn. **64**, 2036 (1995).
[11] M. Toida and Y. Ohsawa, Sol. Phys. **171**, 161 (1997).
[12] M. Toida, T. Suzuki, and Y. Ohsawa, Phys. Plasmas **11**, 3028 (2004).

Downloaded 20 Sep 2007 to 133.6.32.11. Redistribution subject to AIP license or copyright, see http://pop.aip.org/pop/copyright.jsp

[13]T. Kaminura, T. Wagner, and J. M. Dawson, Phys. Fluids **21**, 1151 (1978).
[14]D. E. Baldwin and G. Rowlands, Phys. Fluids **9**, 2444 (1966).
[15]M. Toida, T. Yoshiya, and Y. Ohsawa, Phys. Plasmas **12**, 102306 (2005).
[16]T. D. Kaladze, D. G. Lominadze, and K. N. Stepanov, Sov. Phys. JETP **7**, 196 (1972).
[17]H. Okuda and C. K. Birdsall, Phys. Fluids **13**, 2123 (1970).
[18]Y. L. Klimontovich, *The Statistical Theory of Non-Equilibrium Processes in a Plasma* (MIT Press, Cambridge, MA, 1967).

Downloaded 20 Sep 2007 to 133.6.32.11. Redistribution subject to AIP license or copyright, see http://pop.aip.org/pop/copyright.jsp